Ultrasonic and Brillouin scattering measurements of the elastic constants of BaFCl

1993 J. Phys.: Condens. Matter 5 2749

(http://iopscience.iop.org/0953-8984/5/17/009)

J. Phys.: Condens. Matter 5 (1993) 2749–2758. Printed in the UK

Ultrasonic and Brillouin scattering measurements of the elastic constants of BaFCl

M Fischer†, M Sieskind‡, A Polian§ and A Lahmar†

† Département de Recherches Physiques (Unité associée au CNRS 71), Université Pierre et Marie Curie, T 22, 4 place Jussieu 75252, Paris Cédex 05, France
‡ CNRS Laboratoire Phase, 23 rue du Loess, 67037 Strasbourg Cédex, France
§ Physique des Milieux Condensés (Unité associée au CNRS 782), Université Pierre et Marie Curie, T 13, 4 place Jussieu, 75252 Paris Cédex 05, France

Received 25 November 1992, in final form 5 February 1993

Abstract. The six elastic constants of BaFCl which is a crystal of the matlockite family have been measured using ultrasonic and Brillouin scattering techniques. The values obtained are compared with those of BaF_2 crystals which exhibit some structural similarities with BaFCl. Because of the layer structure of BaFCl, the 'transverse' elastic constants C_{66}, C_{44}, C_{12} and C_{13} and the 'longitudinal' elastic constants C_{33} and C_{11} are smaller than the corresponding constants of BaF_2. The linear and volume compressibilities are deduced from these measurements. An elastic Debye temperature is calculated ($\Theta_{el} = 246.5$ K) and compared with other experimental (calorimetric) and theoretical (shell model) determinations. Finally, the effect of the dipole moments of the halide ions on the elastic constants for materials of the matlockite family is discussed.

1. Introduction

By virtue of their interesting imaging applications, matlockite (PbFCl) structured fluorhalides are of technological importance. Therefore, knowledge of their physical properties is necessary in order to make the best choice of a material for technological applications. In addition, the fluorhalides are interesting from the viewpoint of lattice dynamics because their layer structure, which is derived from the well known fluorite structure, gives them a more or less two-dimensional character. Several experimental and theoretical studies have been published during the last few years, especially in the fields of calculations of cohesive properties [1, 2], lattice dynamics [3, 4] and transport properties based on atomistic simulations [5]. However, to our knowledge, no experimental determination of the elastic constants has been reported. Until now, the only evaluation of the elastic parameters is deduced from a lattice dynamical calculation based on a shell model (SM) [6]. This paper is mainly devoted to the experimental determination of the elastic properties of BaFCl, one of the members of the matlockite family.

BaFCl is a tetragonal crystal which belongs to the D_{4h}^7 space group. Therefore, it is characterized by six independent elastic constants C_{11}, C_{33}, C_{44}, C_{66}, C_{12} and C_{13} which we have measured. C_{33} and C_{44} determine the velocities of phonons propagating parallel to the C_4 axis and C_{11}, C_{12}, C_{44} and C_{66} those of the phonons propagating perpendicular to it. C_{13} appears in the expression for the velocity for intermediate directions.

0953-8984/93/172749+10$07.50

First, the crystal preparation techniques and the measurements performed by using ultrasonic and Brillouin scattering techniques are described. Then, the data are analysed and compared with those of the BaF_2 crystal. The linear and volume compressibilities are calculated. Our results are also compared with those deduced from the SM calculation [6]. Using the values of the elastic constants, an elastic Debye temperature Θ_{el} is calculated using the Voigt–Reuss–Hill–Gilvarny (VRHG) method [7]. This temperature is compared with the value Θ_{cal} deduced from calorimetric measurements and the value Θ(SM) estimated from the SM calculations. Finally, for this antiferroelectric crystal, the effect of the dipole moments of the Cl ions on the elastic constants is discussed. More generally, this effect is discussed with respect to partial results obtained for other compounds of the same family.

2. Experiments

2.1. *Crystal growth*

Single crystals were grown by cooling a melt consisting of an equimolecular mixture of BaF_2 and $BaCl_2$ in a dry argon atmosphere. Details of the growth procedure have been published elsewhere [8]. The crystals reached a volume of about 300 mm^3 and were clear and colourless. Crystal orientation was identified by x-ray diffraction techniques. The samples used in the present experiments were polished parallelepipeds with various dimensions ranging from 2.7 to 6.7 mm. The parallelism of flat opposite faces was better than 1°.

2.2. *Experimental techniques*

2.2.1. Ultrasonic measurements. Four different directions of ultrasonic wave propagation were used: the [100], [110] and [001] directions for the determination of C_{11}, C_{44}, C_{12} and C_{66}. The $[10\bar{1}]$ direction was used to determine a combination of the elastic constants involving C_{13}.

The automated system used to make the ultrasonic velocity measurements was based on the phase quadrature detection method [9]. The resonance frequencies of the transducers were 10 MHz and 5 MHz for the longitudinal and the shear modes, respectively. In these experiments, the absolute value of the acoustic pulse transit time was obtained by repeating the measurements five times on two or three successive echoes. The measured signal resulted from the average of 50 data points. The wave propagation velocity V was deduced from knowledge of this transit time and the path length. Using the value of the density ($\rho = 4.567 \times 10^3$ kg m^{-3}), the elastic moduli ρV^2 and the elastic constants were calculated. The accuracy of the ultrasonic measurements depends on the signal phase quality.

2.2.2. Brillouin scattering measurements. The sample that we used in this experiment had faces perpendicular to the [001], [100] and [010] directions. The main parts of the experimental set-up, which have been described in detail elsewhere [10], were a piezoelectrically scanned five-pass Fabry–Pérot interferometer and a single-mode Ar^+ laser. The wavelength of the exciting light was 514.5 nm. A data accumulation system increased the contrast of the Brillouin peaks. In our experiments, only five to ten data accumulations were required to obtain well defined peaks. Various scattering geometries were used (see table 2). The free spectral angle of the Fabry–Pérot interferometer was 1.364 cm^{-1}.

Table 1. Ultrasonic waves velocities for various propagation and polarization directions.

Propagation direction	Polarization direction	Velocity	Ultrasonic velocity ($m\ s^{-1}$)
[100]	[100]	$\sqrt{\frac{C_{11}}{\rho}}$	3969
[001]	[001]	$\sqrt{\frac{C_{33}}{\rho}}$	3791
[001]	$\perp$	$\sqrt{\frac{C_{44}}{\rho}}$	2112
[100]	[010]	$\sqrt{\frac{C_{66}}{\rho}}$	2282
[110]	$[1\bar{1}0]$	$\sqrt{\frac{C_{11}-C_{12}}{2\rho}}$	2187
[110]	[110]	$\sqrt{\frac{C_{11}+C_{22}+2C_{66}}{2\rho}}$	4068
$[10\bar{1}]$	Quasi-longitudinal	V_+	3936
$[10\bar{1}]$	Quasi-transverse	V_-	2007

Table 2. Brillouin scattering measurements of acoustic waves velocities for various scattering configurations. X, Y, Z indicate respectively the [100], [010] and [001] directions. The configuration $A(B.)D$ indicates that incident and scattered light are along A and D directions respectively, with incident polarization vector parallel to B. The polarization of scattered light is not analysed.

Configuration	Velocity	Value from Brillouin measurement ($m\ s^{-1}$)
$Y(X.)\bar{Y}$	$\sqrt{\frac{C_{11}}{\rho}}$	4078
$Z(X.)\bar{Z}$	$\sqrt{\frac{C_{33}}{\rho}}$	3801
$X(Z.)Y$	$\sqrt{\frac{C_{11}+C_{12}+2C_{66}}{2\rho}}$	3944.5

The Brillouin wavenumber shift $\Delta\sigma$ (cm^{-1}) was related to the sound velocity V by

$$\Delta\sigma = (2nV/\lambda_0 c)\sin(\tfrac{1}{2}\theta) \tag{2.1}$$

where λ_0 and c are the wavelength and the velocity, respectively, of the light in vacuum, θ is the angle between the incident and the scattered light and n is the refractive index at the wavelength of the laser light.

The values of the ordinary refractive index n_o and extraordinary refractive index n_e were deduced previously [8]:

$$n_o = 1.669 \qquad n_e = 1.674.$$

The accuracy of the Brillouin scattering measurements was evaluated without taking into account the accuracy of the refractive index measurement.

2.3. Results

The results of ultrasonic and Brillouin scattering measurements are shown in table 1 and table 2, respectively. Table 3 contains the values of the elastic constants deduced from tables 1 and 2 and the published theoretical values (SM values [6]). The uncertainties in the values of the elastic constants come from the dispersion of the measurements which were repeated on one or several samples. There is good agreement between the ultrasonic and the Brillouin scattering measurements. The discrepancy is 3% at most. The agreement is especially good for C_{33} (2%).

Table 3. Elastic constants of BaF_2 and BaFCl in GPa. $\Delta C/C$ is equal to the ratio of the difference between the calculated and the selected values over the selected value.

Elastic constant (GPa)	Value for BaF_2 [14]	Ultrasound value	Brillouin value	Selected value	Calculated value [6]	$\Delta C/C$ (%)
C_{11}	98	71.9 ± 2.5	75.9 ± 0.2	75.9 ± 0.2	90.8	27
C_{33}	98	65.6 ± 0.2	65.9 ± 0.2	65.7 ± 0.3	60.0	−8
C_{44}	25.4	20.38 ± 0.03		20.38 ± 0.03	24.3	20
C_{13}	44.8	31.9 ± 1.1		31.9 ± 1.1	41.6	30
C_{66}	25.4	23.8 ± 1.1		$23.8 \pm 1/1$	33.2	40
C_{12}	44.8	28.2 ± 1.2		28.3 ± 1.2	26.7	−5

The results of the propagation along the $[10\bar{1}]$ direction are shown in the last two rows of table 1. In this direction, the velocity of a pure shear wave with a polarization vector along the [010] direction is given by

$$V_t = [(C_{44} + C_{66})/2\rho]^{1/2} \tag{2.2}$$

The velocities V_+ and V_- of the quasi-longitudinal and quasi-transverse waves are given by the relations

$$V_\pm = (1/\sqrt{\rho})\left[\tfrac{1}{2}(\Gamma_{11} + \Gamma_{33}) \pm \sqrt{(\Gamma_{11} - \Gamma_{33})^2 + 4\Gamma_{13}^2}\right]^{1/2} \tag{2.3}$$

where Γ_{11}, Γ_{13} and Γ_{33} [11] are related to the elastic constants by

$$\Gamma_{11} = \tfrac{1}{2}(C_{11} + C_{44}) \qquad \Gamma_{13} = \tfrac{1}{2}(C_{13} + C_{44}) \qquad \Gamma_{33} = \tfrac{1}{2}(C_{33} + C_{44}). \tag{2.4}$$

C_{13} is deduced from (2.3) and is given by

$$C_{13} = -C_{44} + \left[(\rho V_+^2 - \rho V_-^2)^2 - \tfrac{1}{2}(C_{11} - C_{13})^2\right]^{1/2}. \tag{2.5}$$

The results presented in table 3 show that the accuracy of the Brillouin scattering measurement of C_{11} is better by an order of magnitude than its ultrasonic determination. The

low accuracy of ultrasonic measurements comes from the small dimension of the samples along the [100] direction (about 3 mm). Consequently we propose for C_{11} the value deduced from the Brillouin experiment, i.e. 75.9 ± 0.2 GPa. On the other hand, the accuracy of the ultrasonic and Brillouin scattering measurements of C_{33} are of the same order of magnitude. Therefore, we suggest for C_{33} a value of 65.7 ± 0.3 GPa which is the mean value of the two measurements.

3. Discussion

3.1. Influence of the crystal structure

Owing to their chemical similarities, it is interesting to compare the crystalline structures of BaFCl and BaF_2. The cubic structure of BaF_2 (figure 1(*a*)) is of fluorine type [12]. Each F^- ion is surrounded by a regular tetrahedron of Ba^{2+} ions. The distance between these two ions is $d_{Ba-F} = 2.68$ Å (table 4). In the BaFCl structure, ionic layers perpendicular to the C_4 axis contain Ba_4F tetrahedra sandwiched between a double layer of Cl^- ions (figure 1(*b*)). In that sense, BaFCl, like the other matlockite-type crystals, may be described as a layer compound even if the interlayer interactions are of the same order of magnitude as the intralayer interactions [13]. The interionic distances are shown in table 4. It is worthwhile noting that the Ba^{2+}–F^- ion distances in the tetrahedron are of almost the same order of magnitude in both structures.

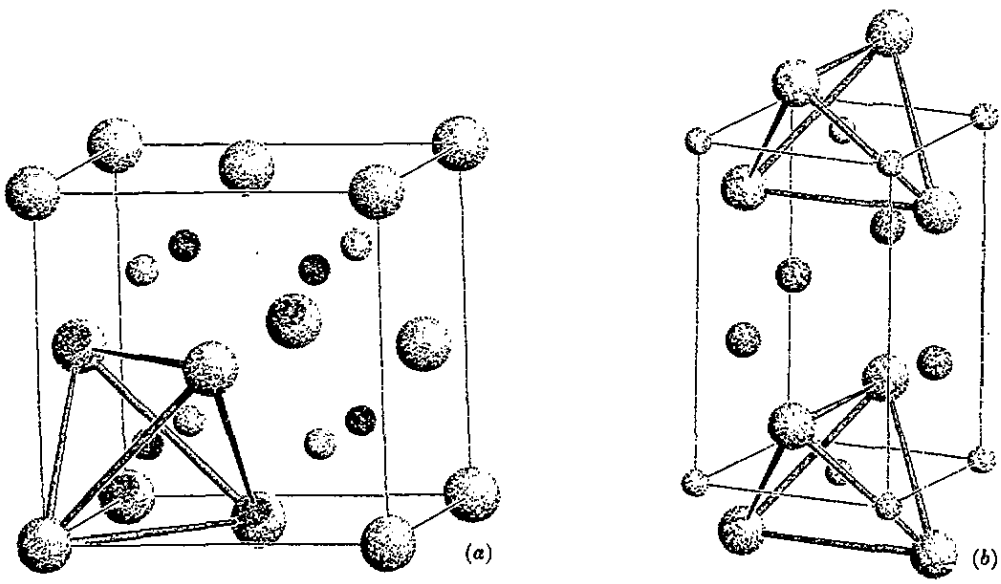

Figure 1. Structures of (*a*) BaF_2 and (*b*) BaFCl.

When these structural considerations are taken into account, the elastic constants of BaFCl can be compared with those of BaF_2 [14]. The elastic constants of BaFCl in

Table 4. Interionic distances (in Å) for MF_2 (M = Ba, Sr) and MFX (X = Cl, Br, I) crystals [12].

	M–F	F–F	X–F	$X–M^I$	$X–M^{II}$	X–X
BaF_2	2.68	4.37				
BaFCl	2.65	3.10	3.36	3.28	3.19	3.76
BaFBr	2.66	3.18	3.44	3.40	3.41	3.88
BaFI	2.69	3.29	3.61	3.58	3.83	4.08
SrF_2	2.5	4.08				
SrFCl	2.49	2.91	3.23	3.11	3.07	3.53

table 3 can be classified into two groups: a 'longitudinal' group L with C_{11} and C_{33} and a 'transverse' group T with C_{66}, C_{44}, C_{12} and C_{13}. The values in a group are roughly similar and are comparable with those of BaF_2. To explain this behaviour as a first approximation, The Ba–F interactions in the tetrahedron should be considered as the strongest and isotropic.

The elastic constants of group L in the cubic crystal BaF_2 are obviously equal. For BaFCl, these constants are related to the linear compressibilities parallel (C_{33}) and perpendicular (C_{11}) to the C_4 axis. As the intralayer and interlayer interactions are of the same order of magnitude, the values of C_{11} and C_{33} are not very different. The intercalation of layers of Cl^- ions between layers of Ba_4F tetrahedra weakens these interactions. Consequently, C_{33} and C_{11} in BaFCl are smaller than C_{11} in BaF_2. The elastic constants of group T are related to the shear, sliding and rotation properties of two adjacent layers. Because of the intercalation of layers of Cl^- ions, these elastic constants in BaFCl are smaller than in BaF_2.

3.2. Compressibilities

In tetragonal crystals, the linear compressibilities and the elastic constants are related by

$$\chi_\parallel = (C_{11} + C_{12} - C_{13})/[C_{33}(C_{11} + C_{12}) - 2C_{13}^2] \tag{3.1}$$

$$\chi_\perp = (C_{33} - C_{13})/[C_{33}(C_{11} + C_{12}) - 2C_{13}^2] \tag{3.2}$$

where the subscripts $\parallel$ and $\perp$ indicate directions parallel and perpendicular to the C_4 axis respectively. In BaFCl, using the present determination of the elastic constants,

$$\chi_\parallel = 8.2 \times 10^{-3}\ \text{GPa}^{-1} \qquad \chi_\perp - 7.2 \times 10^{-3}\ \text{GPa}^{-1}.$$

It is interesting to note that the value of $\chi_\perp/\chi_\parallel = 0.88$ is mainly determined by the ratio $C_{33}/C_{11}(= 0.86)$. The compressional waves along the C_4 axis and the C_2 axis propagate with velocities determined by C_{33} and C_{11}. The value of C_{33}/C_{11} shows that the longitudinal interlayer bonds are slightly weaker than longitudinal intralayer bonds.

The volume compressibility is given by $\chi = \chi_\parallel + 2\chi_\perp$. In BaFCl,

$$\chi = 22.6 \times 10^{-3}\ \text{GPa}^{-1}.$$

This value is consistent with the result obtained by x-ray diffraction measurements [15]:

$$\chi = 24 \times 10^{-3}\ \text{GPa}^{-1}.$$

3.3. Comparison between the calculated and experimental values of elastic constants

The phonon dispersion curves have been calculated using the SM [4]; the six elastic constants were derived from the slope of the acoustic branches (table 3). The calculated values are 20–40% larger than the experimental values (except for C_{33} and C_{12} where they are about 5% smaller). The difference between the calculated values of C_{11} and C_{13} is about 50%. The difference between the calculated values of the elastic constants of group T is larger than that between the measured values.

4. Debye temperature

From the measurement of the elastic constants an elastic Debye temperature Θ_{el} is deduced. Θ_{el} is compared with the value determined using the SM [4, 6] and the value Θ_{cal} obtained by calorimetric measurements [16].

4.1.1. Experimental value of the elastic Debye temperature. From the measurements of the elastic constants, a Debye temperature Θ_{el} may be deduced using VRHG approximation [7]. In this approximation, the Debye model is assumed to be valid and the acoustic waves propagate without dispersion and with an average velocity $\bar{V}_m$. The temperature variations in the density and in the sound velocity are neglected. This approximation is often used, so that the 300 K data are transposed to 0 K. We calculate $\bar{V}_m(0\text{ K}) \simeq \bar{V}_m(300\text{ K}) = 2.36\times10^3\text{ m s}^{-1}$ and

$$\Theta_{el}(0\text{ K}) = 246.5\text{ K}.$$

4.1.2. Experimental value of the calorimetric Debye temperature. A Debye temperature Θ_{cal} was obtained by calorimetric measurements at very low temperatures [16]:

$$\Theta_{cal} = 249\text{ K}$$

This value is in very good agreement with our elastic Debye temperature determination. It can be seen that, for a few hundred compounds, Anderson [17] and Kieffer [7] have found agreement between Θ_{el} and Θ_{cal} of better than 2%. The consistency between these results gives confidence in the specific-heat measurements and those of elastic constants which were made independently.

4.1.3. Theoretical value of the Debye temperature. A theoretical Debye temperature was determined by Balasubramanian and Haridasan [4], using the results of the SM calculations for the phonon density of states and the temperature dependence of the specific heat. There is a large discrepancy between $\Theta_{cal}(SM) = 468.8$ K and Θ_{cal}. This difference can be explained not only by the insufficient accuracy of some IR data used for the SM calculation but also by a computation error.

Indeed, from elastic constants calculated by Balasubramanian *et al* [6] and using the VRHG approximation a theoretical Debye temperature more consistent with its experimental determination is obtained:

$$\Theta_{el}(SM) = 268.4\text{ K}.$$

The results of the different Debye temperature calculations are summarized in table 5.

Table 5. Averaged acoustic waves velocity and Debye temperature.

	Measurement	Calculation
$\bar{V}_m$ (m s^{-1})	2.36 10^{3}[a]	2.57 10^{3}[a,c]
Θ_{el} (K)	246.5[a]	268.4[a]
Θ_{cal} (K)	249[b]	468[c]

[a] Calculated values using the VRHG approximation [7].
[b] From calorimetric measurements.
[c] Calculated from SM [3].

5. Elastic constants and dipole moments

Many compounds of the matlockite family are antiferroelectric. This characteristic is consistent with a D_{4h}^{7} symmetry and with Cl^- ions surrounded by Ba^{2+} ions (figure 1). Antiparallel dipole moments of the Cl^- ions are oriented along the C_4 axis. This antiferroelectric state is responsible for the contribution of the dipolar polarizability to the static dielectric constant [18]. Moreover an order–disorder phase transition has been observed at high temperatures [19].

In order to discuss the effect of these dipole moments on the elastic constant C_{33}, we calculate the dipole moments of some compounds for which C_{33} measurements are available. For BaFCl, data are numerous and the dipole moment μ can be evaluated from the Langevin formula [20]

$$\mu^2 = (3kT/4\pi N_0)\,\Delta\epsilon. \tag{5.1}$$

In this formula, T is the absolute temperature, N_0 the number of permanent dipoles per unit volume and $\Delta\epsilon$ the dipolar contribution to the static dielectric constant. The dipole moment and the Brillouin scattering measurements of the elastic constants C_{33} are shown in table 6.

Table 6. Dipole moment of X^- (Cl^-, Br^-) ion and Brillouin scattering measurement of C_{33} in various MFX crystals.

	μ (D)	C_{33} (GPa)
BaF_2		98
BaFCl	0.6	65.7
BaFBr	$\simeq$1.1	$\simeq$58
BaFI		$\simeq$52
SrF_2		128
SrFCl	>0.8	77

5.1. Discussion

In the BaFX family (X = Cl, Br, I) a decrease in C_{33} is observed from BaFCl to BaFI. This evolution can be correlated with the variation in the interionic distances which induces an increase in the dipole moment. The Ba–F distances are almost constant for all BaFX compounds and the X–X interionic distances increase with increasing X^- ionic radius

(table 4). From chlorine to iodine, the X^- ionic polarizabilities increase proportionally more than the interionic distances. So, the dipole moment of BaFBr is larger than that of BaFCl. Most probably, the following inequalities are correct:

$$\mu(\text{BaFI}) > \mu(\text{BaFBr}) > \mu(\text{BaFCl}).$$

The effect of the dipole moment on the elastic constants has been studied by Frey and Zeyher [21] for PbI_2. Parallel dipoles should induce an increase in C_{33}. On the contrary for MFX compounds it can be foreseen that antiparallel dipoles should induce a decrease in C_{33} and this is shown in table 6.

From similar considerations, one can compare the elastic constants of SrFCl and BaFCl. The dipole moment of the Cl^- ion in SrFCl is larger than in BaFCl because with equal positive charges the distance between M^{2+} and Cl^- ions is shorter. Consequently, the relative decrease in C_{33} with respect to the C_{33}-value in MF_2 should be higher for SrFCl than for BaFCl. This is confirmed in Table 6.

6. Conclusion

The discrepancy between the values of the calculated Debye temperature does question the validity of the SM for describing the behaviour of BaFCl. Indeed, the Debye temperature reflects the strength of the crystalline interatomic forces [22]. The present results and the cohesive energy calculation [1] confirm the predominant ionic nature of the bonds [3], which is the basic foundation of the actual phonon calculations.

However, it would be useful to fit the model parameters again to reproduce the new acoustic, calorimetric and optical data [8, 16]. It will be interesting to complete this theoretical work by studying the effect of model parameter variations on the elastic constants and Debye temperature by including the effect of the dipole moment. Elastic constant and calorimetric measurements are in progress for other matlockite family compounds, especially for SrFCl and BaFI.

Acknowledgments

The authors wish to thank Mrs M Robin and M G Schwalbach (IPCMS) for their technical assistance.

References

[1] Herzig P 1985 *J. Solid State Chem.* **57** 379
[2] Sieskind M and Ayadi M 1983 *J. Solid State Chem.* **49** 188
[3] Balasubramanian K R, Haridasan T M and Krishnamurthy N 1979 *Solid State Commun.* **32** 1095
[4] Balasubramanian K R and Haridasan T M 1981 *J. Phys. Chem. Solids* **42** 667
[5] Baetzolt R C 1987 *Phys. Rev.* B **36** 9182
[6] Balasubramanian K R, Haridasan T M and Krishnamurthy N 1979 *Chem. Phys. Lett.* **67** 530
[7] Kieffer S W 1979 *Rev. Geophys. Space Phys.* **17** 1
[8] Sieskind M, Ayadi M and Zachmann G 1986 *Phys. Status Solidi* b **136** 489

[9] Wallace P M and Garland C W 1986 *Rev. Sci. Instrum.* **57** 3085
[10] Bonello B, Fischer M and Polian A 1989 *J. Acoust. Sci. Am.* **86** 225
[11] Dieulesaint and Royer D 1974 *Ondes Élastiques dans les Solides* (Paris: Masson)
[12] Wyckoff R 1963 *Crystal Structure* vol 1 (New York: Wiley–Interscience)
[13] Bärnighausen H, Brauer G and Schultz N 1965 *Z. Anorg. (Allg). Chem.* **338** 250
[14] Gerlich D 1964 *Phys. Rev.* A **135** 1331
[15] Beck H P, Limmer A, Denner W and Schulz H 1983 *Acta Crystallogr.* B **39** 401
[16] Dossmann Y, Kuentzler R, Sieskind M and Ayachour D 1989 *Solid State Commun.* **72** 377
[17] Anderson O L 1963 *J. Phys. Chem. Solids* **24** 909
[18] Ayachour D, Sieskind M and Geist P 1991 *Phys. Status Solidi* b **166** 43
[19] Sieskind M, Ayachour D and Fettouhi A 1993 to be published
[20] Fröhlich H 1948 *Theory of Dielectrics* (Oxford: Oxford University Press)
[21] Frey A and Zeyher R 1978 *Solid State Commun.* **28** 435
[22] Brüesch P 1982 *Theory and Experiments* vol 1 (Berlin: Springer)